

BEAUTY AND CHARM PRODUCTION CROSS SECTION MEASUREMENTS AT THE TEVATRON

J.M. PURSLEY

on behalf of the CDF and DØ Collaborations

*Physics Department, Room 2320 Chamberlin Hall, University of Wisconsin-Madison,
1150 University Avenue, Madison, WI 53706, USA*



Heavy quark production probes QCD at the interface of the perturbative and non-perturbative regimes. Studying the production of heavy quarks is an important test of models in both regimes. In this article, recent results on beauty and charm production from the CDF and DØ experiments at the Tevatron are reported. These include measurements of correlated $b\bar{b}$ production, the $\psi(2S)$ production cross section, and $\Upsilon(1S)$ and $\Upsilon(2S)$ polarization.

1 Introduction

The study of heavy quark production is an important test of models of both perturbative and non-perturbative quantum chromodynamics (QCD). Since the development of nonrelativistic QCD (NRQCD), the agreement between theoretical predictions and measured values of heavy quark production cross sections has improved greatly. However, recent J/ψ and $\psi(2S)$ polarization measurements at the Tevatron¹ indicate the understanding of heavy quark production is not yet complete.

The Tevatron at the Fermi National Accelerator Laboratory produces $p\bar{p}$ collisions with a center of mass energy of 1.96 TeV. The Collider Detector at Fermilab (CDF) and DØ experiments employ general multipurpose detectors^{2,3} to reconstruct particle physics events from these collisions. With b -hadron cross sections of $\sim 30 \mu\text{b}$ ($|\eta| < 1.0$),^{2,4} CDF and DØ have a wealth of experimental data on b -hadrons.

2 Correlated $b\bar{b}$ Production

The cross section for producing, in hadronic collisions, both the b and \bar{b} quarks centrally and above a given p_T threshold is referred to as the $b\bar{b}$ correlation $\sigma_{b\bar{b}}$. The exact next-to-leading order (NLO) prediction of $\sigma_{b\bar{b}}$ appears to be a robust perturbative QCD prediction, differing by only a few percent from the leading order (LO) prediction. However, Run I measurements of $\sigma_{b\bar{b}}$ at the Tevatron are inconclusive, with an average ratio of the measured $\sigma_{b\bar{b}}$ over the exact NLO prediction (R_{2b}) of 1.8 with a 0.8 RMS deviation.⁵

In this measurement,⁶ $\sigma_{b\bar{b}}$ is obtained in 740 pb⁻¹ of CDF data using dimuon events with $p_T(\mu) > 3$ GeV/ c , $|\eta| < 0.7$, and invariant mass $m_{\mu\mu} \in [5, 80]$ GeV/ c^2 . This corresponds to $b\bar{b}$ pairs with $p_T \geq 2$ GeV/ c and rapidity $|y| \leq 1.3$. At the Tevatron, dimuon events mainly result from the decay of heavy quark pairs ($b\bar{b}$ or $c\bar{c}$), the Drell-Yan process, the decay of charmonium and bottomonium, and the decay or misidentification of π or K mesons. To determine the $b\bar{b}$ and $c\bar{c}$ content of the data, we fit the impact parameter distribution of the muon tracks. The impact parameter d_0 is defined as the distance of closest approach of the track to the primary event vertex in the transverse plane, and it is proportional to the decay time of the parent particle.

The one-dimensional impact parameter distributions of muons from b and c decays are modeled by a tuned Herwig simulation,⁶ while the distributions of prompt muons are reconstructed using muons from $\Upsilon(1S)$ decays in the data. Because the impact parameters of the two muons are to first order uncorrelated, the three 1D templates may be combined into six 2D templates to represent each possible dimuon source ($b\bar{b}$, $c\bar{c}$, cb , prompt-prompt, prompt- b , and prompt- c). These six templates are then used to perform a maximum likelihood fit to the 2D distribution of the impact parameter of both muons to extract the $b\bar{b}$ and $c\bar{c}$ components. The projection of the 2D impact parameter distribution is compared to the fit result in Figure 1.

From this fit, we measure the dimuon cross sections to be $\sigma_{b \rightarrow \mu, \bar{b} \rightarrow \mu} = 1549 \pm 133$ pb and $\sigma_{c \rightarrow \mu, \bar{c} \rightarrow \mu} = 624 \pm 104$ pb, where the quoted error is the sum in quadrature of statistical and systematic uncertainties. In order to compare with theoretical predictions, we evaluate the NLO dimuon cross section using the MNR generator with the events decayed by EvtGen.⁶ This gives a value of $\sigma_{b \rightarrow \mu, \bar{b} \rightarrow \mu}^{\text{NLO}} = 1293$ pb, resulting in a ratio of $R_{2b} = 1.2 \pm 0.2$. This measurement is in agreement with the NLO theoretical prediction, and does not confirm the anomalously high dimuon cross section observed in Run I.

3 $\psi(2S)$ Production Cross Section

Charmonium production provides another arena in which to test our understanding of QCD. The development of NRQCD was prompted in part by the CDF Run I measurements of J/ψ and $\psi(2S)$ production cross sections.⁷ A new CDF measurement of the $\psi(2S)$ production cross section pushes the p_T range farther into the perturbative QCD regime than was possible with Run I data.⁸

We reconstruct $\psi(2S) \rightarrow \mu^+\mu^-$ using 1.1 fb⁻¹ of CDF data. We then perform an unbinned maximum likelihood fit in the $\psi(2S)$ mass and proper decay length ct distributions. The mass fit separates the signal from the background, while the ct fit separates promptly-produced $\psi(2S)$ from $\psi(2S)$ originating from secondary decays of long-lived particles (predominantly B mesons). The $\psi(2S)$ p_T range of 2 to 30 GeV/ c is divided into 25 bins, and the signal yield and prompt fraction in each p_T bin are extracted by the likelihood fit.

The $\psi(2S)$ acceptance depends upon the $\psi(2S)$ polarization. The CDF measurement of $\psi(2S)$ polarization is statistically limited, with only three measured data points.¹ We take the average of these three data points as the effective polarization $\alpha_{\text{eff}} = 0.01 \pm 0.13$, where α is defined according to Equation (1), and use this value to calculate the $\psi(2S)$ acceptance in each

bin of $\psi(2S)$ p_T .

The final result is shown in Figure 2, where the promptly produced $\psi(2S)$ are separated from those produced in B decays. The CDF Run I measurement is also shown in Figure 2. The integrated cross section has increased by $18 \pm 19\%$ from the Run I measurement, compared to a theoretical prediction of $14 \pm 8\%$ for the change in center of mass energy from 1.80 TeV to 1.96 TeV.⁸ The integrated inclusive differential cross section is measured to be

$$\begin{aligned} \sigma(p\bar{p} \rightarrow \psi(2S)X, |y(\psi(2S))| < 0.6, p_T > 2\text{GeV}/c)_{\sqrt{s}=1.96\text{TeV}} \cdot Br(\psi(2S) \rightarrow \mu^+\mu^-) \\ = 3.17 \pm 0.04(\text{stat.}) \pm 0.28(\text{syst.}) \text{ nb.} \end{aligned}$$

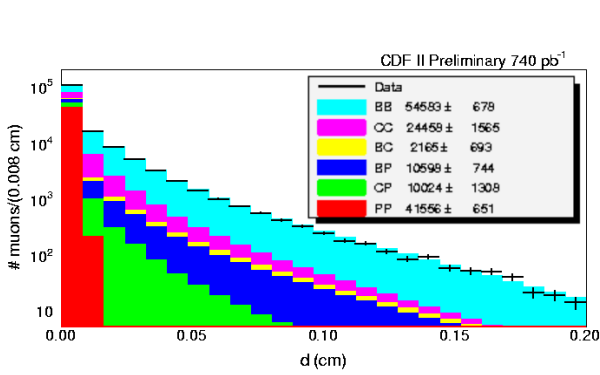


Figure 1: Projection of the two-dimensional impact parameter distribution of muon pairs compared to the result of a fit for the $b\bar{b}$ and $c\bar{c}$ components. The different letter combinations in the legend indicate the dimuon source, as explained in the text: “B” for a muon from a b quark, “C” for a muon from a c quark, and “P” for a prompt muon. The legend gives the number of events found by the fit for each dimuon source, along with the statistical uncertainty.

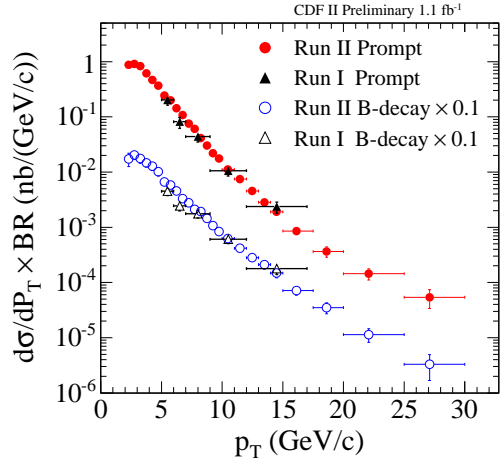


Figure 2: The differential cross section for prompt $\psi(2S)$ (solid circles) and $\psi(2S)$ from B meson decays (hollow circles). The cross section for $\psi(2S)$ from B meson decays is scaled down by a factor of 10 so that the two curves may be seen separately. Triangular markers indicate the results of a CDF Run I measurement, which has not been scaled to account for the difference in center of mass energy.⁷

4 Polarization of $\Upsilon(1S)$ and $\Upsilon(2S)$

Recent measurements of the J/ψ and $\psi(2S)$ polarization at CDF show significant longitudinal polarization with increasing p_T ,¹ while NRQCD predicts transverse polarization at sufficiently high p_T for S -wave quarkonia produced in $p\bar{p}$ collisions. Now $D\mathcal{O}$ presents new measurements of the $\Upsilon(1S)$ and $\Upsilon(2S)$ polarization, another important test of the theoretical approaches to QCD.

The polarization is measured in the parameter α , defined as:

$$\alpha = \frac{\sigma_T - 2\sigma_L}{\sigma_T + 2\sigma_L} \quad (1)$$

where σ_T and σ_L are the transverse and longitudinally polarized components of the cross section respectively. If the transverse and longitudinal states are equally populated, one measures $\alpha = 0$; for longitudinal polarization, $\alpha < 0$, while for transverse polarization, $\alpha > 0$. In quarkonia decay to a lepton and anti-lepton, α may be obtained from the angular distribution

$$\frac{dN}{d(\cos\theta^*)} \propto 1 + \alpha \cos^2\theta^* \quad (2)$$

where θ^* is the angle between the Υ in the lab frame and the positive lepton in the Υ rest frame.

Using 1.3 fb^{-1} of $D\bar{O}$ data, we find 420 000 $\Upsilon(nS) \rightarrow \mu^+\mu^-$ candidates.⁹ The Υ data are divided into several bins in Υp_T (p_T^Υ) and $|\cos\theta^*|$, and the number of $\Upsilon(1S)$ and $\Upsilon(2S)$ in each bin are extracted from a fit to the Υ mass distribution. The mass signal consists of three peaks, the $\Upsilon(1S)$, $\Upsilon(2S)$, and $\Upsilon(3S)$, where the mass differences between the peaks are fixed to the measured values.¹⁰ Unfortunately, the number of $\Upsilon(3S)$ was insufficient to extract the angular distributions. The angular distribution in each bin is compared to $\Upsilon(1S)$ and $\Upsilon(2S)$ Monte Carlo samples which were generated with the parameter α set to zero. The measured value of α for the data is then determined by reweighting the angular distributions in the Monte Carlo. The dependence of α on p_T^Υ is plotted in Figure 3 for both $\Upsilon(1S)$ and $\Upsilon(2S)$, along with various theoretical predictions. While statistics for the $\Upsilon(2S)$ are insufficient to draw a conclusion, in the $\Upsilon(1S)$ there is significant p_T dependent longitudinal polarization which is only marginally consistent with any of the theoretical predictions.

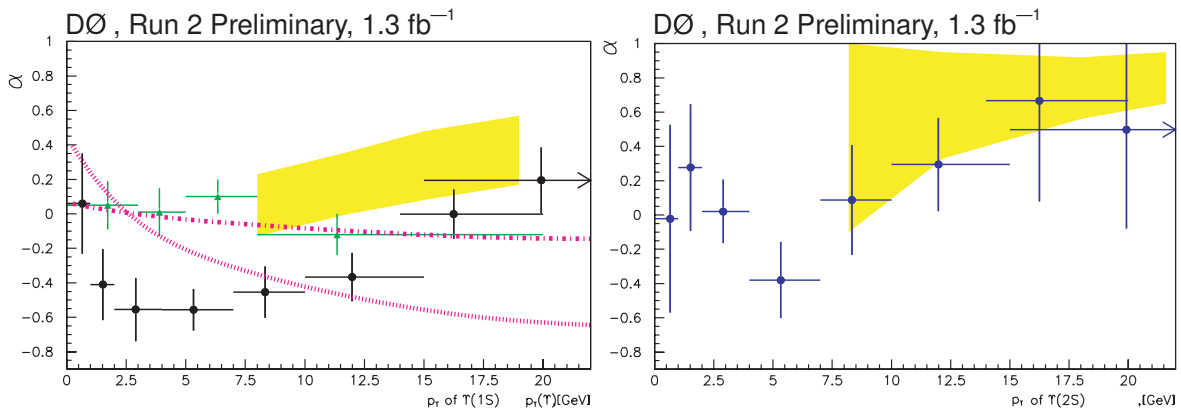


Figure 3: On the left is shown the dependence of the polarization parameter α on p_T^Υ for the $\Upsilon(1S)$. The black points are the $D\bar{O}$ data, while the green triangles are the CDF Run I result.¹¹ The yellow band corresponds to an NRQCD prediction,¹² while the two dashed curves are two limiting cases from k_T factorization models.¹³ The lower line corresponds to the quark-spin conservation hypothesis, while the upper line corresponds to the full quark-spin depolarization hypothesis. On the right is shown the dependence of α on p_T^Υ for the $\Upsilon(2S)$. The blue points are the $D\bar{O}$ data and the yellow band is an NRQCD prediction.

5 Conclusions

Recent measurements of the $b\bar{b}$ correlation and the $\psi(2S)$ cross section at the Tevatron are in agreement with NLO and NRQCD predictions. However, measurements of quarkonia polarization in the same perturbative p_T regime show discrepancies from theoretical predictions. Theoretical models are now challenged to match the polarization measurements while continuing to describe the cross section data.

Acknowledgments

We thank the Moriond QCD organizers for the invitation to attend this conference, and are grateful for the receipt of a travel grant from the European Union Marie Curie Program. We also thank the Fermilab staff and the technical staffs of the participating institutions for their vital contributions to this work, as well as the funding agencies supporting this work.

References

1. A. Abulencia *et al.* (CDF Collaboration), *Phys. Rev. Lett.* **99**, 132001 (2007).
2. D. Acosta *et al.* (CDF Collaboration), *Phys. Rev. D* **71**, 032001 (2005).
3. V. Abazov *et al.* (DØ Collaboration), *Nucl. Instrum. Methods A* **565**, 463 (2006).
4. The detectors use a cylindrical coordinate system with the z -axis along the proton beam direction. Rapidity is denoted by y , while the pseudorapidity η is defined as $\tanh^{-1}(\cos \theta)$. Transverse momentum, p_T , is the component of the particle momentum in the (x, y) plane.
5. F. Happacher, P. Giromini, and F. Ptohos, *Phys. Rev. D* **73**, 014026 (2006).
6. T. Aaltonen *et al.* (CDF Collaboration), submitted to *Phys. Rev. D* (*Preprint hep-ex/0710.1895*).
7. F. Abe *et al.* (CDF Collaboration), *Phys. Rev. Lett.* **79**, 572 (1997).
8. CDF Collaboration, CDF Note 9074 (2007) and references therein, <http://www-cdf.fnal.gov/physics/new/bottom/071018.blessed-psi2S-xsec>.
9. V. Abazov *et al.* (DØ Collaboration), submitted to *Phys. Rev. Lett.* (*Preprint hep-ex/0804.2799*).
10. W. M. Yao *et al.* (Particle Data Group), *J. Phys. G* **33**, 1 (2006).
11. D. Acosta *et al.* (CDF Collaboration), *Phys. Rev. Lett.* **88**, 161802 (2002).
12. E. Braaten and J. Lee, *Phys. Rev. D* **63**, 071501 (2001).
13. S. P. Baranov and N. P. Zotov, *Pis'ma v ZhETF* **86**, 499 (2007) (*Preprint hep-ph/0707.0253*).